ChemComm

Synthesis and Characterization of Cell-Microenvironment-sensitive Leakage-free Gold-shell Nanoparticle with template of Interlayer-Crosslinked Micelle

Journal:	*ChemComm*
Manuscript ID:	CC-COM-03-2015-002556.R2
Article Type:	Communication
Date Submitted by the Author:	28-Apr-2015

Complete List of Authors:	Dai, Jian; School of Engineering, Sun Yat-sen University, Li, Qianqian; School of Engineering, Sun Yat-sen University Guangzhou, China, Liu, Wenya; School of Engineering, Sun Yat-sen University, Hao, Yaoyao; School of Engineering, Sun Yat-sen University, Lin, Shudong; School of Chemistry and Chemical Engineering, Sun Yat-sen University Guangzhou, China, Zhang, Chao; School of Engineering, Sun Yat-sen University Guangzhou, China Guangzhou, China, Shuai, Xintao; School of Chemistry and Chemical Engineering, Sun Yat-sen University,

Journal Name

RSCPublishing

COMMUNICATION

Synthesis and Characterization of Cell-Microenvironment-sensitive Leakage-free Gold-shell Nanoparticle with template of Interlayer-Crosslinked Micelle

Cite this: DOI: 10.1039/xoxxoooooox

Received ooth January 2012,
Accepted ooth January 2012

DOI: 10.1039/xoxxoooooox

www.rsc.org/

Jian Dai,[a,*] Qianqian Li,[a] Wenya Liu,[a] Shudong Lin,[b] Yaoyao Hao,[a] Chao Zhang[a] and Xintao Shuai[b]

The novel gold-shell nanoparticles (pH-GSNPs) are firstly designed, which exhibits drug leakage-free behavior at physiological environment, while achieves rapid drug release and remarkable aggregation for the nanogold interlayer of pH-GSNPs to shift their absorption to far-red and NIR as a photothermal agent at intracellular microenvironment.

Recently, there has been a burst of activity on the design and engineering of plasmonic nanostructures[1-3] for photothermal therapy[4-8] and drug delivery[9-17]. Much work has thus gone into the development of gold nanostructures for the combination therapeutic of cancer phototherapy and chemotherapy. Gold nanocages covered by temperature-responsive polymers for drug delivery could release pre-loaded drugs in a controllable fashion using a near-infrared laser.[18] Gold nanocontainers for spatially and temporally controlled drug delivery was leakage-free over extended storage, and responsive to light irradiation, and offers an important mechanism for monitoring drug release profiles.[19] To facilitate combined doxorubicin and photothermal treatments, doxorubicin-loaded poly(lactic-co-glycolic acid)-gold half-shell nanoparticles were developed by depositing Au films on DOX-loaded PLGA NPs, resulting in higher therapeutic efficacy and shorter treatment times.[20,21]

At present, there are two ways to prepare organic/inorganic hybrid nanogold self-assembly. Firstly, the bottom-up design of hierarchical nanogolds derives from the self-assembly of amphiphilic gold nanoparticles.[7-9,22] This plasmonic self-assembly structurally resembles polymer micelles or vesicles and facilitates biomedical applications in bioimaging and photothermal therapy of cancer. Secondly, the top-down method is addressed from in-situ formation of gold-"decorated" self-assembly by using nano-templates, such as micelles, nanoparticles, or vesicles.[19-21,23] However, the thermodynamic instability of these templates limits the scope of this approach. Recently, using star-like block copolymers as nanoreactors that are structurally stable, therefore overcomes the intrinsic instability of linear block co-polymer micelles and enables the facile synthesis of nearly monodisperse nanocrystals. [24]

Herein, we described the first example of pH-tunable leakage-free gold-shell nanoparticles (pH-GSNPs) for pontential photothermal therapy and drug delivery, with the stable template of the highly packed interlayer-crosslinked micelles (HP-ICMs) from the triblock copolymer, mPEG-*b*-PAsp(MEA)-*b*-PAsp(DIP)[25] (Fig. S1. and S2., supporting information). The preparation mechanism and pH-tunable performance by Transmission electron microscopy (TEM) was studied, and loaded Doxorubicin (DOX) release profile was evaluated by using UV-vis, and the intracellular location of pH-GSNPs was analyzed by using confocal laser scanning microscopy (CLSM) and TEM. More importantly, pH-GSNPs could dissociate at low pH (pH 5.0) and form aggregates, and the intracellular-microenvironment-induced aggregates shifted their absorption to far-red and NIR. Hence, our pH-GSNPs revealed the great potential of delivering both heat and drug to tumorigenic regions, and they may improve the therapeutic effectiveness with minimal side effects.

Recent work has shown that thiol-containing amphiphilic copolymers are capable of acting as stabilizing agents to perform thiol-stabilized AuNPs by using interfacial ligand-exchange method.[7,22] As such, the triblock copolymer, mPEG-*b*-PAsp(MEA)-*b*-PAsp(DIP) with a thoil residue block could act as the stabilizing agent of AuNPs. However, compared to the previous method, we presented in-situ formation of gold shell displaying the disulfide interlayer of HP-ICMs. Hence, the pH-GSNPs were synthesized using HP-ICMs as dimensional confinements/stabilizing agents. Meanwhile, certain secondary and tertiary amine-containing polymers are also capable of acting as stabilizing agents.[26] Therefore, the triblock copolymer using in the present study has two kinds of in situ stabilizing agents (i.e., thiol and tertiary amine of residue blocks), respectively existed in the interlayer and core of HP-ICMs. Since the preparation system is highly complex, the study of pH-GSNPs' preparation mechanism is strongly needed.

Due to elucidating the preparation mechanism and pH-sensitivity of pH-GSNPs, as shown in Fig. 1 and Fig. 2, we designed the procedure for the synthesis of pH-GSNPs with a strong reduction agent (e.g., $NaBH_4$) and a weak reduction agent (e.g., NH_2OH) and studied the morphology of pH-GSNPs for the proofs that how the gold nanostructure would be stabilized by using thiol or tertiary residue of HP-ICMs at different pH (i.e., pH = 5.0, 7.4, and 10.0).

Unlike previous in-situ approaches, the two kinds of stabilizing agents are designed to serve the purpose for forming gold nanostructure, and the final morphology of pH-GSNPs would directly relate to the performance of drug controlled release, due to the pH-sensitive core with encapsulating hydrophobic drugs (e.g.,

doxorubicin, paclitaxel, and et al).

The HP-ICMs at pH 7.4 PBS buffer solution currently prepared retain the stabilizing agents (i.e., thiol and tertiary amine of residue blocks) in the interlayer and core of HP-ICMs, allowing for subsequent reduction of ionic gold salt (e.g., $NaAuCl_4$) by using $NaBH_4$. The synthesis procedure of pH-GSNPs is depicted in Fig. 1. In Fig. 1, the HP-ICMs at pH 7.4 PBS buffer solution was chosen to prepare the pH-GSNPs at the same pH, through adding 50 μL, 0.1mg/mL $NaAuCl_4$ and $NaBH_4$ solution in sequence.

Our previous results indicate that the pH-sensitive DIP groups (pKa≈6.4) can tune the PAsp(DIP) core soluble or insoluble or partially soluble by controlling pH of the whole solution.[25] So adjusting pH from 7.4 to 10.0 and 5.0, the pH-GSNPs at pH 10.0 and 5.0 were prepared for evaluating the internalization of gold nanostructure in the pH-GSNPs. From TEM micrographs showed in Fig. 1, the pH-GSNPs at pH 7.4 had a diameter of 100-150 nm and formed the morphology of "gold nanocages" in the interlayer of the HP-ICMs with the partial hydrated cores. On the other hand, since the high hydrophobicity of PAsp(DIP) at pH10.0 formed the solid core of pH-GSNPs, the morphology of the pH-GSNPs at pH 10.0 shinked to form "gold nanoparticles" with a diameter of 80-100 nm from "gold nanocages" of the pH-GSNPs. Thus, it strongly suggests that thoil residue of the HP-ICMs forms more stable gold-thiolate bonds, compared to tertiary amine residue in polymeric core of the HP-ICMs. This observation is supported by the previous report.[27] However, when the core polymer PAsp(DIP) of the pH-GSNPs became completely soluble at pH5.0, the force for core expansion was much stronger. Therefore, the gold shell of the pH-GSNPs got to collapse, due to the fact that the partially hydrophobic polymeric core transformed into the totally hydrophilic cavity so as to hardly support the gold shell morphology of pH-GSNPs. Therefore, pH-GSNPs as drug carriers could be used to deliver hydrophobic drugs for controlled release related to cancer cell microenvironment.

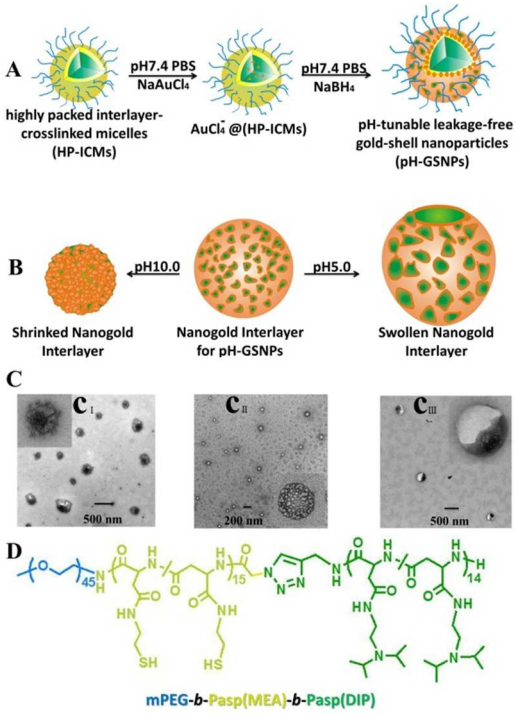

Fig. 1. Preparation and characterization of pH-tunable leakage-free gold-shell nanoparticles (pH-GSNPs), not stained with uranyl acetate. (A) Schematic plot of pH-GSNPs preparation with the template of highly packed interlayer-crosslinked micelles (HP-ICMs) from the triblock copolymer mPEG-*b*-Pasp(MEA)-*b*-Pasp(DIP) by using a reduction agent, $NaBH_4$ and 50 μL $NaAuCl_4$ with concentration of 0.1 mg/mL at pH 7.4 solution, at constant amount of HP-ICMs (1 mL, 1 mg/mL at pH 10.0); (B) pH-tunable morphology transformation of nanogold interlayer for pH-GSNPs at different pH, with forming shrinked nanogold interlayer at pH 10.0 and swollen nanogold interlayer at pH 5.0; (C) Transmission electron microscopy (TEM) images of the nanogolds, not stained with uranyl acetate, at pH values of a) 10.0, b) 7.4, c) 5.0.

The present method for gold nanostructure synthesis relies on gold ligand competence between thiol and tertiary amine. As such, NH_2OH was used as the weak reduction agent for addressing nanogold in the interface interlayer of pH-GSNPs. The pH-GSNPs were fabricated [50 μL $NaAuCl_4$ volume with concentration of 1 mg/mL at pH 7.4; NH_2OH volume with 50% content is equal to $NaAuCl_4$ volume at constant amount of HP-ICMs (1 mL, 1 mg/mL at pH 10.0)]. From TEM micrographs in Fig. 2A, the pH-GSNPs at pH10 were clearly composed of a large number of 10 nm nanogold and exhibited spherical morphology of closely attached nanogolds self-assembly. It could be observed that the nanogolds existed in the interior and periphery of the pH-GSNPs. However, Adjusted to pH7.4, the nanogolds significantly aggregated in the periphery of the pH-GSNPs with the shell thickness of about 20 nm (Fig. 2B). Therefore, it figures out that the nanogolds mainly dispersed in the interlayer of the pH-GSNPs. And the contrast between the core and shell was significantly enhanced because of the settlement of 10 nm nanogolds in the shell. Since pH-sensitive core of the pH-GSHPs became completely soluble at pH5.0, the force for core expansion was much stronger. Therefore, the spherical morphology of the pH-GSNPs got to expand and collapse, as depicted in Fig. 2$C_{II}$and C_{III}. When continued to add GSH at pH5.0, the morphology of pH-GSHPs had disappeared and the nanogolds considerably aggregated in a form of random (Fig. 2D).

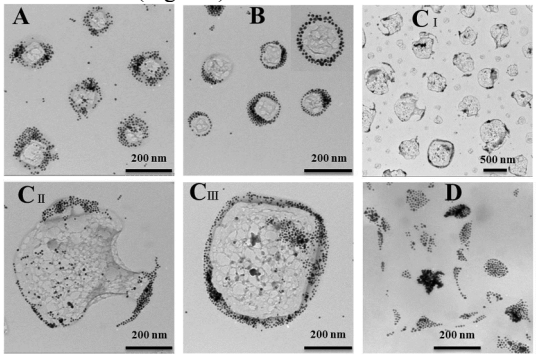

Fig. 2. Transmission electron microscopy (TEM) images for addressing nanogold in the interface interlayer of pH-GSNPs by using a reduction agent NH_2OH, not stained with uranyl acetate. (A) at pH10; (B) at pH7.4; (C_{I-III}) at pH5.0, C_{II} and C_{III}: High resolution TEM images of individual nanoparticle; (D) add 10mM GSH at pH5.0. 50 μL $NaAuCl_4$ with concentration of 1 mg/mL at pH 7.4 solution, at constant amount of HP-ICMs (1 mL, 1 mg/mL at pH 10.0); NH_2OH volume with 50% content is equal to $NaAuCl_4$ volume. Adjust pH by using 0.1g/ml HCl from the same sample at pH10.

After elucidating the preparation mechanism and pH-sensitivity of pH-GSNPs, we used two-stage process for drug-loaded pH-GSNPs: the first stage is to prepare Au seed nanoparticles shown in Fig. 2, and then Au nanoshell growth is formed for pH-GSNPS using Au seed nanoparticles shown in Fig. 3S and Fig. 3.

The pH-GSNPs were designed to study the effect of the amount of

$NaAuCl_4$ on their morphology (size, shape, and dispersibility). Since the morphology of pH-GSNPs exhibited a strong dependence on $NaAuCl_4$ volume currently added. Therefore, for preparing the gold nanoshell of pH-GSNPs, gold seed nanoparticles are firstly prepared on the interlayer of HP-ICMs and gold nanoshells are then grown around the interlayer of pH-GSNPs. No significant difference at particle dispersibility with diameters of 100 nm (Fig. 3S: A) was seen in contrast to pH-GSNPs with diameters from 200 nm to largely irregular size (Fig. 3S: B, C, and D) that significantly aggregated. It figures out that the hydrophilic poly(ethylene glycol) can disperse pH-GSNPs with confined gold shells (such as Fig. 3S: A). However, the $NaAucl_4$ content needed to be controlled and otherwise, gold nanostructures with solid-core would possibly be formed and didn't dissociate to release the encapsulated drugs in intracellular microenvironment, e.g. low pH and glutathione (GSH) and et al.

In the present study, the proper amount ratio of $NaAuCl_4$ and HP-ICMs [(1 μL for gold seed nanoparticles + 50 μL for gold nanoshell growth): 1 mL at the constant concentration of 1 mg/mL pH7.4 PBS] was chosen to prepare pH-GSNPs (showed in Fig. 3A) with significant dispersibility for drug delivery. Meantime, when adjusting pH 5.0 from pH7.4, it was found that the core polymer PAsp(DIP) became completely soluble and the force for core expansion was much stronger. And then the nanostructure of pH-GSNPs dissociated and gold nanoparticle residues currently available participated self-assembly to form "gold nanoworms" (Fig. 3B). And then it came to aggregate with adding GSH that exists in cells. A possible explanation for this behavior could be attributed to the carboxyl anionic interactions with tertiary amine cation formed at pH5.0[28,29] (Fig. 3C).

Since most gold nanoparticles have their optical resonances in the visible range, the resonances need to be engineered to longer wavelengths before they can be successfully used for anticancer photosensitizers. Recently, gold nanoparticles tethered with organic compounds or polymers have emerged as a new class of building blocks for the fabrication of various superstructures with interesting optoelectronic properties. For example, the ″smart″ gold nanoparticles could respond to pH change and form aggregates, and the pH-induced aggregates shift their absorption to far-red and NIR.[30] In the present study, due to the fact that the low pH value and reducing agent GSH exist inside lysosomes of cells, the absorption spectra of pH-GSNPs (Fig. 3C) were examined at different conditions. Initially, pH-GSNPs showed their absorption peak at 550 nm at pH7.4 PBS. The pH5.0 solution from pH-GSNPs at pH7.4 PBS showed a red shift of the absorption with broadening. Broadening is ascribed to the appearance of coupled plasmon modes and inhomogeneity of the aggregates.[19,30] When adding GSH into the pH5.0 solution, the absorption peak shifted down to 700-800 nm with its red side tail broadening over 800 nm. This is clearly indicative of intracellular microenvironment sensitive aggregation of pH-GSNPs. This promises that the interactions between charged nanoparticles can prevail in intracellular environment where various interferences by electrostatic attractions with biomolecules are expected.

The pH-sensitive release for encapsulated drugs from pH-GSNPs was evaluated by directly determining the amount of released DOX using the conventional UV-vis analysis in Fig. 4A. Notably, DOX release from the pH-GSNPs at neutral pH was hardly detected in the experiment up to 24 h, which indicates that no DOX leakage from the pH-GSNPs may be effectively avoided in neutral physiological environments containing almost no reductive agent, e.g. in blood. In the meantime, immediate acceleration of DOX release was observed using single stimulus of adjusting the solution pH to 5.0, while the most remarkable "burst release" of DOX was determined when dual stimuli were applied simultaneously. Moreover, no significant distinction was seen at pH5.0 and pH5.0 solution with adding GSH. In the latter case, almost 40% of the encapsulated drug was released within 5 h. Since the experimental conditions in our release study has been set up to mimic the environment inside lysosomal compartments, i.e. the pH value around 5.0 and existence of the reductive agent GSH, the results should imply that our pH-GSNPs may rapidly release the encapsulated DOX after entering the cells via endocytosis and being entrapped inside lysosomes, as will be more clearly shown in cell culture study as well.

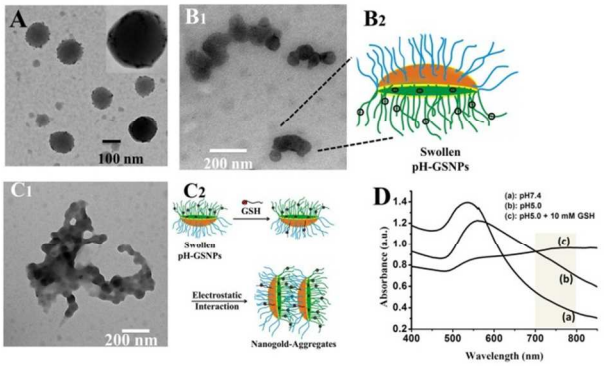

Fig. 3. Transmission electron microscopy (TEM) images of the pH-GSNPs at pH7.4 by using a reduction agent NH_2OH (A) and schematic plot of swollen pH-GSNPs at pH 5.0 (B_1 and B_2) and aggregation morphology of swollen pH-GSNPs at pH 5.0 by adding GSH (C_1 and C_2); Visible/NIR spectra for pH-GSNPs at different conditions (D) with the proper amount ratio of $NaAuCl_4$ with concentration of 1 mg/mL (1 μL for gold seed nanoparticles + 50 uL for gold nanoshell growth), NH_2OH as a reduction agent and 1 mL HP-ICMs at the constant concentration of 1 mg/mL pH7.4 PBS, not stained with uranyl acetate.

It is well known that free DOX is a nuclei-targeted drug and thus can enter the nuclei in a short time, whereas DOX transported by conventional non-sensitive micelles accumulated in nuclei very slowly.[25] In the present study, two experimental time points (2 h and 6 h) via endocytosis were chosen to study Intracellular DOX release profile. As shown in Fig. 4B, after 2 h via endocytosis, DOX fluorescent absorbance of the pH-GSNPs in the cells was very weak and a rapid nucleic accumulation of DOX was not detected, indicating that most DOX molecules were not released yet from the pH-GSNPs. It may be because the pH-GSNPs were intact and there existed a fluorescence quenching effect of DOX molecules which were embedded at relatively high density in the gold shell of pH-GSNPs. In contrast, after cells were incubated for 6h, a fast accumulation of DOX in nuclei was observed. It can be concluded that the pH-GSNPs was transformed to a dissociating structure (Fig. 3B and C.) upon decreasing the solution pH, DOX turned into water-soluble upon reprotonation and diffused much more easily inside the pH-GSNPs core. These factors are in favor of a rapid release of DOX from the pH-GSNPs, leading to an obvious increase in DOX fluorescent intensity. The rapid release of DOX from the pH-GSNPs inside SKOV-3 cells is consistent with the data obtained in the release study in buffered solutions. Based on these results, we believe that the low pH value (around 5.0) and reductive agent GSH inside lysosomes have caused disassembly of the pH-GSNPs, resulting in the fast lysosomal release and nucleic accumulation of DOX. As shown in Fig. 4C, after SKOV-3 cells were incubated for 6h, the data by using high-resolution TEM clearly achieved the endocytosis mechanism for pH-GSNPs uptake. The gold nanostructures of the pH-GSNPs could be observed in the endosome

with low pH and the obvious aggregation like "gold nanoworms" illustrated drug release from the pH-GSNPs. Therefore, the results are consistent with that by adding GSH and pH5.0. And it is able to be used to in vivo photothermal cancer therapy.

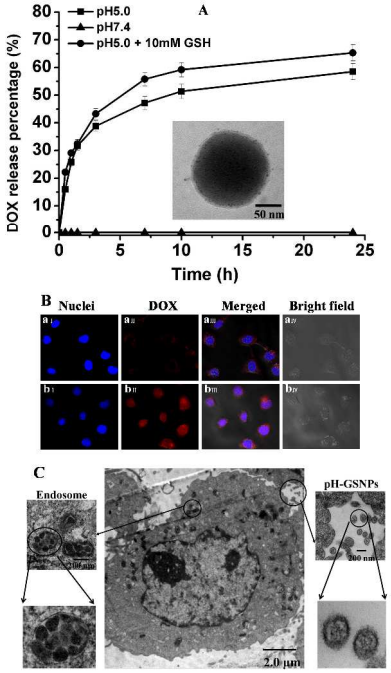

Fig. 4. (A) Quantitative DOX release from pH-GSNPs (mean±standard deviation (SD), n=3); (B) Intracellular DOX release and migration into nuclei observed by CLSM. SKOV-3 cells were incubated (37 ℃) for 2 h (a) and 6 h (b) at a DOX-equivalent dosage of 10 mg per dish. DOX loading contents: 10.5% in pH-GSNPs. Nuclei were stained with Hoechst 33342 (blue); (C) TEM analysis of the intracellular location of pH-GSNPs internalized into SKOV-3 cells. Magnified images of organelles are shown alongside. The black dots inside endosomes are pH-GSNPs. Cells were incubated for 6 h.

In summary, pH-GSNPs exhibited structural stability, drug leakage-free behavior in blood circulation, and had no absorption to far-red and NIR; while at intracellular microenvironment, the gold-shell of pH-GSNPs dissociated and rapidly release encapsulated drugs. More importantly, the nanogold interlayer of pH-GSNPs could remarkably aggregate to shift their absorption to far-red and NIR of 700-800nm, and it would be used as photothermal agents. And at the present, we are studying pH-GSNPs for targeted drug delivery and photothermal therapy to integrin-rich tumors. Our results mean that pH-GSNPs designed exhibit attractive potential for synergetic therapeutic efficacy with chemotherapy and photothermal therapy.

Acknowledgements

The authors thank the financial support of the National Natural Science Foundation of China (No. 21104097) and Natural Science Foundation of Guangdong Province (No. 2014A030313152) and the Fundamental Research Funds for the Central Universities of China (No. 12lgpy01) and Guangdong Innovative Research Team Program (No. 2009010057).

Notes and references

[a] School of Engineering, Sun Yat-sen University, Guangzhou 510006, P. R. China. E-mail: daijian@mail.sysu.edu.cn

[b] School of Chemistry and Chemical Engineering, Sun Yat-sen University, Guangzhou 510006, P. R. China

† Electronic Supplementary Information (ESI) available: [details of any supplementary information available should be included here]. See DOI: 10.1039/c000000x/

1 S. Eustis and M. A. El-Sayed, *Chem. Soc. Rev.*, 2006, **35**, 209.
2 C. M. Cobley, J. Chen, E. C. Cho, L. V. Wang, Y. Xia, *Chem. Soc. Rev.*, 2011, **40**, 44.
3 A. N. Shipway, E. Katz, I. Willner, *ChemPhysChem*, 2000, **1**, 18.
4 E. C. Cho, Y. Liu, Y. Xia, *Angew. Chem. Int. Ed.*, 2010, **49**, 1976.
5 H. Wang, D. W. Brandl, P. Norlander, N. J. Halas, *Acc. Chem. Res.*, 2007, **40**, 53.
6 J. Chen, M. Yang, Q. Zhang, E. C. Cho, C. M. Cobley, C. Kim, C. Glaus, L. V. Wang, M. J. Welch, Y. Xia, *Adv. Funct. Mater.,* 2010, **20**, 3684.
7 J. He, X. L. Huang, Y. C. Li, Y. J. Liu, T. Babu, M. A. Aronova, S. J. Wang, Z. Y. Lu, X. Y. Chen, Z. H. Nie, *J. Am. Chem. Soc.*, 2013, **135**, 7974.
8 J. He, Y. J. Liu, T. Babu, Z. J. Wei, Z. H. Nie, *J. Am. Chem. Soc.*, 2012, **134**, 11342.
9 Jibin Song, Jiajing Zhou, Hongwei Duan. J. Am. Chem. Soc. 2012, 134, 13458−13469.
10 Zhao, W. A.; Karp, J. M. *Nat. Mater.*, 2009, **8**, 453.
11 M. R. Jones, J. E. Millstone, D. A. Giljohann, D. S. Seferos, K. L. Young, C. A. Mirkin, *ChemPhysChem*, 2009, **10**, 1461.
12 S. E. Lee, G. L. Liu, F. Kim, L. P. Lee, *Nano Lett.*, 2009, **9**, 562.
13 G. B. Braun, A. Pallaoro, G. H. Wu, D. Missirlis, J. A. Zasadzinski, M. Tirrell, N. O. Reich, *ACS Nano*, 2009, **3**, 2007.
14 D. V. Volodkin, A. G. Skirtach, H. Mohwald, *Angew. Chem., Int. Ed.*, 2009, **48**, 1807.
15 T. S. Troutman, S. J. Leung, M. Romanowski, *Adv. Mater.*, 2009, **21**, 2334.
16 D. A. Giljohann, D. S. Seferos, W. L. Daniel, M. D. Massich, P. C. Patel, C. A. Mirkin, *Angew. Chem. Int. Ed.*, 2010, **49**, 3280.
17 B. Kim, G. Han, B. J. Toley, C. Kim, V. M. Rotello, N. S. Forbes, *Nat. Nanotechnol.*, 2010, **5**, 465.
18 M. S. Yavuz, Y. Cheng, J. Chen, C. M. Cobley, Q. Zhang, M. Rycenga, J. Xie, C. Kim, K. H. Song, A. G. Schwartz, L. V.Wang, Y. Xia, *Nat. Mater.*, 2009, **8**, 935.
19 Y. Jin and X. Gao, *J. Am. Chem. Soc.*, 2009, **131**, 17774.
20 H. Park, J. Yang, J. Lee, S. Haam, I. H. Choi, K. H. Yoo, *ACS Nano*, 2009, **3**, 2919.
21 H. Park, J. Yang, S. Seo, K. Kim, J. Suh, D. Kim, S. Haam, K. H. Yoo, *Small*, 2008, **4**, 192.
22 J. Hu, T. Wu, G. Zhang, S. Liu, *J. Am. Chem. Soc*., 2012, **134**, 7624.
23 J. Kim, S. Park, J. E. Lee, S. M. Jin, J. H. Lee, I. S. Lee, I. Yang, J.-S. Kim, S. K. Kim, M.-H. Cho, T. Hyeon, *Angew. Chem. Int. Ed. 2006*, **45**, 7754.
24 X. Pang, L. Zhao, W. Han, X. Xin, Z. Lin, *Nat. Nanotechnol.* 2013, **8(6)**: 426-31.
25 J. Dai, S. Lin, D. Cheng, S. Zou, X. Shuai, *Angew. Chem. Int. Ed.*, 2011, **50**, 9404.
26 M. A. Nash, J. J. Lai, A. S. Hoffman, P. Yager, P. S. Stayton, *Nano Lett.*, 2010, **10**, 85.
27 J. Love, L. Estroff, J. Kriebel, R. Nuzzo and G. Whitesides, *Chem. Rev.*, 2005, **105**, 1103.
28 R. Hong, G. Han, J. M. Fernández, B. Kim, N. S. Forbes, V. M. Rotello, *J. Am. Chem. Soc.* 2006, **128**, 1078.
29 B. Kim, G. Han, B. J. Toley, C. K. Kim, V. M. Rotello, N. S. Forbes, *Nat Nanotechnol.* 2010, **5(6)**:465.
30 J. Nam, N. Won, H. Jin, H. Chung, S. Kim, *J. Am. Chem. Soc.*, 2009, **131**, 13639.

